Modal analysis of waveguide for the study of frequency bandgaps of a bounded periodic medium

Michaël Darche, Fernando Lopez-caballero, Bing Tie

Modal analysis of waveguide for the study of frequency bandgaps of a bounded periodic medium

M. Darche[a], F. Lopez-Caballero[a], B. Tie[a,*]

[a] *Université Paris-Saclay, CentraleSupélec, ENS Paris-Saclay, CNRS, LMPS - Laboratoire de Mécanique Paris-Saclay, 91190, Gif-sur-Yvette, France.*

Abstract

A novel method based on waveguide modal analysis is presented to evaluate the effectiveness in terms of frequency bandgaps of bounded periodic metamaterials. The effect of the size of the bounded medium, i.e., the number of periodic unit cells, on the frequency bandgaps predicted by Floquet-Bloch theory in the infinite case is investigated and quantified. The waveguides considered in this work have a bounded cross-section and an infinite longitudinal axis simulated by Perfectly Matched Layers. Its useful area is made of a bounded 1D or 2D-periodic matrix-inclusion metamaterial. In the 2D-periodic case, an approach combining the waveguide modal analysis with the Floquet-Bloch transform is further proposed. Applying the proposed method, the SH-waves propagating in a waveguide are studied by using the finite element method. The discrete spectrum of the waveguide and the associated attenuated or trapped wave modes are calculated and analyzed, which provides, within a semi-analytic framework, an exact characterization regarding the attenuation coefficient and the frequency bandgaps of the studied bounded periodic medium. More particularly, effectiveness indicators are defined to compare the width and the position of frequency bandgaps between the bounded and infinite cases as a function of the cell number. Last but not least, the proposed method is also successfully applied to bounded periodic media with local resonators to characterize their filtering and attenuation effectiveness, which shows its interest in such a case of great practical interest.

*Corresponding author

Email address: bing.tie@centralesupelec.fr (B. Tie)

Keywords: Metamaterials; Floquet-Bloch theory; Seismic waves; Modal analysis; Waveguides; Bounded periodic medium;

1. Introduction

In order to reduce the induced damage from waves generated principally by ambient vibrations or earthquakes in structures (e.g., the ones designed before the implementation of seismic standards), a promising strategy is to reduce the amplitude of seismic waves by locally treating the subsoil to modify its mechanical characteristics [1–13, among others]. Avilés and Sánchez-Sesma [14] show that it is possible to modify and reduce the seismic energy distribution for appropriately selected frequency ranges to limit the damage to the structure. In practice, the principal solution is the installation of multiple rows of barriers between a vibration source and the area of protection. Among the various types of barriers, trenches, solid or hollow piles are often used. These kind of solutions is commonly called seismic metamaterials.

Previous numerical and experimental works have been conducted in order to estimate the amplitude reduction or the shielding effectiveness as a function of both the mechanical and geometric characteristics of the inclusion (e.g., diameter, shape, solid or hollow, material properties' contrast between inclusion and soil matrix), the number of rows, the distance between two rows compared to the wavelength of the incomings waves [1, 6, 15–20, among others]. However, to measure the effectiveness of such a protection system, it is necessary to study the wave diffraction phenomena within a bounded domain made of periodic material [21].

In practice, the dispersive characteristics of a periodic medium with respect to the propagation of elastic waves are usually studied within the framework of an infinite domain using the Floquet-Bloch (F-B) theory [17, 18, 22–26, among others]. The F-B transform makes it possible to reduce the analysis of the behavior of an infinite periodic media to the modal analysis of a single elementary unit cell. In the published studies, the key point concerns the assessment of both the geometrical and mechanical parameters of the periodic rows of pile/trench barriers on the apparition of filtering/attenuation frequency ranges (also named bandgaps). Therefore, due to the fact that actually, the number of periodic matrix-inclusion cells is limited to a finite number, the identified beneficial properties of the assumption of an infinite domain, such as the existence of frequency bandgaps and their characteris-

tics (e.g., width and center frequency), must be double-checked against the dimension of the bounded periodic domain [26–28].

Several numerical parametric studies have been conducted in order to assess the differences between these two hypotheses [20, 29–31]. Previous works on soil media subjected to surface waves principally evaluate the effectiveness of a periodic medium as a function of the number of elementary cells or rows that compose the barriers by comparing the values of the attenuation in the frequency bandgaps [18, 25, 32, 33, among others]. They have been mostly focused on the direct use of the finite element method (FEM) or the boundary element method (BEM) to understand the isolation mechanism of wave barriers. Most of them can be qualified as measurement-based, i.e., with a chosen recording zone separated by wave barriers from the sources, they define an amplitude reduction factor in terms of the ratio between surface displacement or acceleration amplitude with and without wave barriers. However, an issue with this factor is that it does not provide an exact characterization of wave barriers; for instance, it depends on the chosen studied zone and is generally not uniform, so an averaged amplitude reduction factor must be defined. Another issue concerns the meshing complexity associated with elastic properties discontinuities due to the barrier inclusions and the large size of the numerical model imposed by the number of propagated wavelengths, which drastically increases the computation time. As an example, Jenson studied in [34] the vibrational response of finite 1-D and 2-D mass-spring periodic lattice structures subjected to periodic loadings. One of his results is to show the convergence of the response in the bandgap frequency range as a function of the unit cell number by considering the frequency response functions (FRF) of the structure recorded at the end of the finite periodic barrier. He studied, in the 1D case, a periodic structure composed of up to 10 unit cells and, in the 2D case, up to 7x7 unit cells. In the 2D case, only the case of loadings concentrated at a point is considered and the finite periodic structure is characterized by the FRF response at only one point located on the other side. Furthermore, the mass-spring framework of Jenson's study cannot be easily extended to periodic structures exhibiting complex microstructural geometry.

Thus, in order to assess for a bounded periodic metamaterial the effectiveness of the analytically predicted frequency bandgaps using the F-B theory, a novel method based on the waveguide modal analysis is proposed in this work. The waveguides considered in this work have a bounded cross-section and an infinite longitudinal axis which is simulated with Perfectly

Matched Layers (PMLs) [35, 36, among others]. The waveguide modal analysis method was initially developed and used to highlight modes trapped by irregularities [37–40] or to find defects in the propagation media [41, 42]. In this paper, this approach is extended and adapted to characterize a heterogeneous bounded periodic medium, e.g., its discrete spectrum, and attenuated or trapped modes. Hence, in contrast to the measurement-based direct numerical modeling, the proposed approach provides exact characterization, within a semi-analytic framework, in terms of attenuation coefficient and bandgaps for the studied problem.

Applying the proposed method, parametric studies can be carried out so as to quantitatively assess both the filtering and attenuation effectiveness of bounded periodic systems, which should converge to the modal solution of the F-B analysis when the system becomes infinite. Indeed, wave modes in a bounded periodic medium are calculated and characterized, and the effect of the latter's size (i.e., the number of cells) on their attenuation or filtering is quantified regarding both the position and width of bandgaps compared with those of the corresponding infinite domain predicted by the F-B theory.

Otherwise, in many practical applications, it is also important to limit the size of periodic cells (especially in the case of urban installations). However, Bragg scattering bandgaps have their frequency ranges directly linked to the size of periodic cells. Thus, to obtain bandgaps at frequencies much lower than those expected by the Bragg diffraction phenomenon, local resonance bandgaps were introduced [43], which have since aroused great interest, for instance, in the field of civil engineering for the design of metabarriers. The proposed waveguide-base modal analysis approach is also applied to bounded periodic media with local resonators to characterize their filtering and attenuation effectiveness.

The outline of the paper is as follows. In Section 2, after the definition of the model problem considered in this study and a brief introduction of the Floquet-Bloch theory, the modal analysis of waveguides is presented, and its extension to a bounded periodic domain is proposed. In Section 3, using the proposed waveguide-based approach, the numerical investigation of bounded 1D-periodic media, *i.e.*, periodic media with a periodicity in one direction, is conducted and compared to the infinite case. In Section 4, to study a 2D-periodic medium, *i.e.*, a periodic medium with a periodicity in two directions, a new strategy to combine the F-B theory and the waveguide method is presented. Then again, parametric studies are carried out to characterize the studied bounded 2D-periodic medium. Finally, Section 5 applies the

proposed method to a bounded 1D-periodic matrix-inclusion medium with local resonators and shows its interest in this case of great practical utility.

2. Model wave propagation problem and modal analysis of waveguides applied to bounded periodic media

The model problem considered herein is the propagation of SH waves in an elastic medium Ω, which is governed by the following equation in the frequency domain:

$$\nabla_{\boldsymbol{x}} \cdot \big(\mu(\boldsymbol{x}) \nabla_{\boldsymbol{x}} u(\boldsymbol{x})\big) = -\rho\omega^2 u(\boldsymbol{x}). \tag{1}$$

where $\boldsymbol{x} = x_1\boldsymbol{e}_1 + x_2\boldsymbol{e}_2$, $u(\boldsymbol{x}) \equiv u_z(\boldsymbol{x})$ is the out-of-plane displacement reduced to a scalar component, and $\mu(\boldsymbol{x})$ and $\rho(\boldsymbol{x})$ are respectively the shear modulus and the density.

In this study, it is assumed that the model problem Eq.(1) is defined in a 2D periodic medium, infinite or bounded. More particularly, a medium with periodically located circular inclusions is considered without loss of generality (Figure 1).

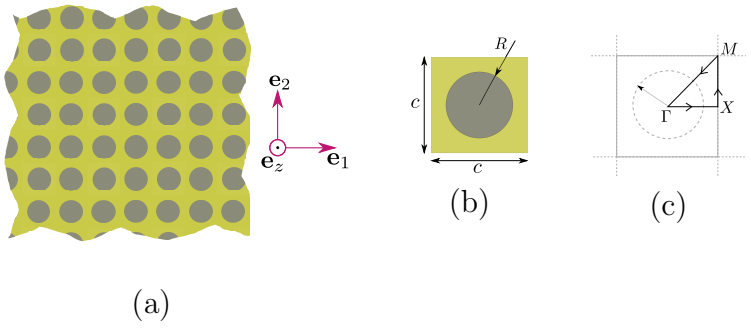

Figure 1: (a) A 2D-periodic medium with unit cells consisting of a matrix and a circular inclusion; (b) Unit cell Q_0 in physical space; (c) Corresponding reciprocal cell, the first Brillouin zone Q^0 in reciprocal space, on which the contour of the Brillouin irreducible zone, $\Gamma \to X \to M \to \Gamma$, is represented.

In the case of an infinite periodic medium, the analysis of its dispersion properties is usually performed using the F-B transform, which makes it possible to reduce the analysis of the behavior of an infinite periodic media to the modal analysis of a single unit cell, denoted Q_0 hereafter (Figure 1(b) for

an example of Q_0 composed of a matrix and an inclusion for the 2D studied case in the present work). Indeed, the F-B transform of a non periodic function $u(\boldsymbol{x})$ defined on Ω reads as:

$$U^B(\boldsymbol{x},\boldsymbol{k}) = \sum_{\{m_j\}\in Z^d} u(\boldsymbol{x} + \sum_{j=1,d} m_j \boldsymbol{g}_j) e^{i\boldsymbol{k}.(\boldsymbol{x}+\sum_{j=1,d} m_j \boldsymbol{g}_j)} \tag{2}$$

with $\{\boldsymbol{g}_j\}_{j=1,d}$ the basis of periodicity vectors of Ω, in the present work $d = 1$ or 2. In Eq.(2), $\boldsymbol{k} \in Q^0$, is the Bloch wave vector that evolves in the reciprocal space limited to Q^0 the Brillouin irreducible zone (Figure 1(c) for an example of Q^0 for the 2D studied case in the present work).

Applying the Floquet-Bloch transform Eq.(2) to Eq.(1) gives rise to the following eigenvalue problem:

$$(\nabla_{\boldsymbol{x}} + i\boldsymbol{k}) \cdot \big(\mu(\boldsymbol{x})(\nabla_{\boldsymbol{x}} + i\boldsymbol{k})U^B(\boldsymbol{x},\boldsymbol{k})\big) = -\rho(\boldsymbol{x})\omega^2 U^B(\boldsymbol{x},\boldsymbol{k}) \tag{3}$$

then, dispersion surfaces $\omega(\boldsymbol{k})$ can be obtained by solving this eigenvalue problem for the wave vector $\boldsymbol{k} \in Q^0$. Furthermore, if Eq.(3) is solved only for the wave vector $\boldsymbol{k}$ belonging to the contour of the irreducible Brillouin zone, dispersion curves are obtained instead [44].

For the eigenvalue problem Eq.(3) defined on the unit cell Q_0, it is generally necessary to use numerical methods to calculate its solutions. Then, the dispersion curves of the medium under consideration can be plotted. In the present work, for a given value of $\boldsymbol{k}$, the computed eigenvalue is $\omega^2(\boldsymbol{k})$, solved using the commercial finite element code, Comsol-Multiphysics. The dispersion curves obtained from infinite periodic media will serve as reference results, useful for comparison studies with bounded periodic media.

A real protection system exploiting a periodic medium is generally not infinite, and the modal characterization of such a bounded system cannot be done with the F-B transform approach. To characterize such a bounded system, surrounded by an infinite domain like the soil, a temporal analysis could be done. However, depending on the size of the bounded periodic medium to be considered and the number of cells, the numerical simulation becomes very expensive due to the fact that the element size must be refined with respect to the characteristic length of heterogeneities.

Now, a method based on the waveguide modal analysis [37, 39, 40] is proposed. It provides a semi-analytic solution for the bounded system surrounded by an infinite domain. It allows a quantitative assessment of the filtering and attenuation effectiveness of bounded periodic systems, which

should converge to the modal solution of the F-B analysis when the system becomes infinite.

The waveguides considered in this work are a system that allows waves to be guided and has a bounded cross-section and an infinite longitudinal axis. One of the methods to study this family of waveguides is the simulation of infinite media using Perfectly Matched Layers (PMLs) [35, 36, among others]. The main idea is based on the fact that the modes obtained by modal analysis of a waveguide could describe both the behavior of the infinite medium and the defects included in a localized zone. Thanks to the use of the PMLs, it is possible to separate the modes corresponding to the behavior of the medium at infinity from those localized because trapped and/or attenuated due to the presence of local defects.

Therefore, the first goal of this section is to distinguish the modes corresponding to the behavior of the infinite medium and those trapped and/or attenuated by a bounded periodic medium containing a finite number of cells.

2.1. Elements of the spectral theory for waveguides including a specific zone of interest

In this part, some basic elements of the spectral theory for partial differential operators are provided. Let us consider the eigenvalue problem of a waveguide with a specific zone of interest governed by an equation of type:

$$\mathbb{A}(\mathbf{u}) = \lambda \mathbf{u} \tag{4}$$

where $\mathbb{A}$ is a self-adjoint linear operator. The specific zone is the one that contains irregularities and breaks the homogeneity of the waveguide. For the studied case defined by Eq.(1), we have $\lambda = \omega^2$ and $\mathbb{A}(\mathbf{u}) = -\frac{1}{\rho}\nabla_{\boldsymbol{x}} \cdot \big(\mu(\boldsymbol{x})\nabla_{\boldsymbol{x}} u(\boldsymbol{x})\big)$.

The modal analysis of a waveguide allows the calculation of the spectrum of the operator $\mathbb{A}$, denoted $\sigma(\mathbb{A})$, which is the complement of the set of complexes $\rho(\mathbb{A})$, the resolvent set of $\mathbb{A}$, defined as:

$$\rho(\mathbb{A}) = \{\Lambda \in \mathbb{C}, \mathbb{A} - \Lambda\mathbb{I} \text{ is invertible}\}. \tag{5}$$

For a bounded system, $\sigma(\mathbb{A})$ is in fact the set of eigenvalues defined as:

$$\sigma(\mathbb{A}) = \{\lambda \in \mathbb{C}, \mathbb{A}\mathbf{u} = \lambda\mathbf{u} \text{ et } \mathbf{u} \neq \mathbf{0}\} \tag{6}$$

However, for an open system like the waveguide, it is considered that $\mathbb{A}$ is an unbounded operator. Therefore, it is not always possible to have equality

for the eigenvalue system, but only a limit. This is the case of the essential spectrum of $\mathbb{A}$, denoted $\sigma_{ess}(\mathbb{A})$ and defined below.

Indeed, the spectrum $\sigma(\mathbb{A})$ can be decomposed into two sets: $\sigma_{disc}(\mathbb{A})$ the discrete spectrum (i.e., the set consisting of all the isolated eigenvalues of the spectrum) and $\sigma_{ess}(\mathbb{A})$ the essential spectrum (i.e., the complement of σ_{disc} in the spectrum):

$$\sigma_{ess}(\mathbb{A}) = \{\lambda \in \mathbb{C}, \mathbb{A} - \lambda\mathbb{I} \text{ is not a Fredholm operator of index } 0\} \quad (7)$$

Then, the behavior of the waveguide is studied by separating $\sigma_{disc}(\mathbb{A})$ from $\sigma_{ess}(\mathbb{A})$. To accomplish this, the idea is to use the PMLs to represent the infinite waveguide. It consists of performing a change of geometric variables to complex that directs the essential spectrum in the complex plane and reveals the discrete eigenvalues distributed on or around the real axis. Hence, the modal analysis of waveguides allows the differentiation between the discrete spectrum of the modes in the bounded domain, which is interesting for the study, and the essential spectrum of the modes in the PMLs, which represent the infinite medium (i.e., the geometrical configuration of the waveguide).

The modes describing the solution of the wave propagation inside the PMLs are not considered in the following. The domain of interest being in the bounded domain, only the discrete spectrum modes are considered in the sequel.

In this work, so as to perform the modal analysis of the studied waveguide, contrary to the usual definition of PMLs [35, 45], the properties in the subdomains represented by the PMLs are independent of the wave frequency [46]. This modification eliminates the frequency dependence of the mass and stiffness matrices, making modal analysis possible.

2.2. Configuration of the bounded periodic matrix/inclusion medium with a waveguide approach

As recalled before, in this work the approach is applied to quantitatively characterize a bounded periodic matrix/inclusion medium. The aim is to quantify the effect of the finiteness of the periodic medium on its filtering properties and to overcome the limitation of the F-B theory that is only capable of dealing with an infinite number of cells.

For this purpose, a 1D waveguide model of a total length L_{tot} and with a finite number n_{cells} of matrix/inclusion unit cells is defined (Figure 2). The

central part of the waveguide is the domain of interest of length L_u, also called the useful area, which is delimited on both sides by two PMLs of length L_{PML}. The useful area is made up of n_{cells} cells in its center and a marginal zone of length L_m on each side:

$$L_{tot} = L_u + 2L_{PML} \ , \ L_u = n_{cells}c + 2L_m \tag{8}$$

The role of the marginal zones between the edge of the bounded periodic medium and the PMLs is to limit the effects of the periodic medium on the PMLs. The different parameters, L_{tot}, L_u, L_m, and L_{PML}, need to be adjusted and are presented below.

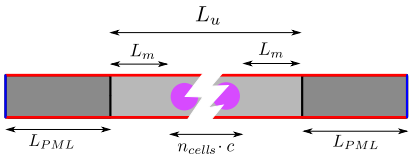

Figure 2: 1D waveguide model composed of: 1) a useful area of length L_u, which contains, at the center, n_{cells} matrix-inclusion unit cells of size c consisting of a matrix (light grey) and a circular inclusion (purple), and at each end, a marginal zone of length L_m; 2) two PMLs (dark gray) of length L_{PML}, with free boundary conditions (on red edges) and clamped boundary conditions (on blue edges).

As stated above, the PMLs are used, and they are defined through the following change of variables to complex [39]:

$$\chi_\theta(x_1) = \begin{cases} -\dfrac{L_u}{2} + (x_1 + \dfrac{L_u}{2})e^{\eta^{left}} & \text{if } x_1 \leq -\dfrac{L_u}{2} \\ x_1 & \text{si } |x_1| < \dfrac{L_u}{2} \\ +\dfrac{L_u}{2} + (x_1 - \dfrac{L_u}{2})e^{\eta^{right}} & \text{si } x_1 \geq \dfrac{L_u}{2} \end{cases} \tag{9}$$

where $\eta^{left/right} = \pm i\theta$ allows to choose the rotation of the essential spectrum in the complex plane. In the following, the two PMLs are said to be conjugated if they are defined such that $\eta^{left} = \overline{\eta^{right}}$, while in the case where $\eta^{left} = \eta^{right}$, they are said to be classical. In an arbitrary way having no impact on the results, we choose $\eta^{left} = -i\theta$. In what follows, the results are mainly obtained with conjugated PMLs, unless it is explicitly stated that classical PMLs are used.

As previously mentioned, contrary to the usual properties of PMLs, the damping of the absorbing layer does not depend on the frequency (i.e., θ is

independent of the frequency). The change of variables in Eq.(9) modifies the differential operator of the problem Eq.(1) only in the PMLs. The resolution of the eigenvalue problem associated with the modified operator then consists of two parts, one giving the modal solutions of the finite problem, (i.e., in the area where the bounded periodic medium is located), and the other concerning the modal response of the PMLs.

2.3. Spectrum and characteristic modes in a homogeneous waveguide

In the following, for the numerical simulations, the geometry parameters and the material properties of the studied periodic media are given in Table I. They are chosen to be more in agreement with the Civil Engineering applications. For instance, inclusions are more rigid than the matrix, and c the unit cell's size is equal to 1 m, which corresponds to what is feasible in practice.

c (m)	R (m)	μ_m (GPa)	μ_i (GPa)	ρ_m (kg/m^3)	ρ_i (kg/m^3)
1	0.346	0.233	30	1750	2400

Table I: Summary of the data used for the simulation of the 2D-periodic medium, where subscripts "m" and "i" represent the soil matrix and the inclusions, respectively.

The Figure 3 represents the case of a uniform waveguide (i.e., a waveguide without any matrix-inclusion cells). The homogeneous material behavior is defined by the shear modulus μ_m and mass density ρ_m while the elastic inclusion by corresponding quantities μ_i and ρ_i (Table I). The dimensions chosen for this homogeneous waveguide are $L_{tot} = 40$ m, $L_u = 20$ m, and $L_{PML} = L_u/2 = 10$ m. In the following, we choose to always have $L_{PML} = L_u/2$. The solution of this homogeneous case serves as a reference to see the evolution of the behavior of the waveguide when a bounded periodic medium is added and to account for new phenomena.

In summary, two types of modes are observed in the homogeneous waveguide. The first type groups the modes associated with complex eigenvalues belonging to $\sigma_{ess}(\mathbb{A})$ the essential spectrum of the operator $\mathbb{A}$ (displayed in black in the Figure 3), which is directed in the complex plane because of the definition of the PMLs. These modes evolve in the PMLs, and an example of them is given in the Figure 4(a). The change of variable to complex performed in PMLs modifies the geometry to model an infinite domain by a finite model. The parameter θ in Eq.(9) is, in fact, the angle made in the

complex plane by the first branch of the essential spectrum with the real axis (which corresponds to the spectrum in an infinite homogeneous domain).

The second type groups are the modes associated with real eigenvalues (displayed in cyan in the Figure 3), and an example of them is shown in the Figure 4(b). These modes are propagative within the useful area without attenuation or reflection. They are evanescent in the PMLs because of their complex part. Indeed, without heterogeneity, waves propagate in the waveguide without attenuation or reflection, which results in real eigenvalues. For numerical simulation, an eigenvalue ω is considered a real number when its imaginary part is between -0.01 and 0.01.

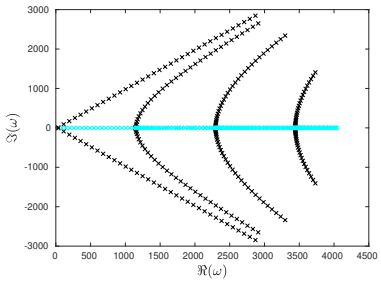

Figure 3: Spectrum of the homogeneous waveguide in the complex plane: σ_{disc} with real eigenvalues (cyan) and σ_{ess} (black).

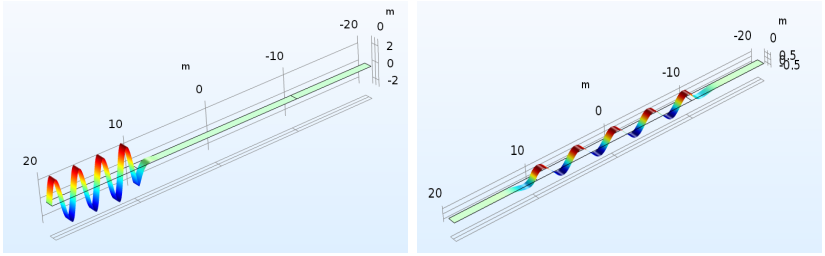

(a) (b)

Figure 4: Two types of modes in a homogeneous waveguide modeled using PMLs. (a) Propagative mode contained in PMLs; (b) Propagative mode in the useful area without reflection or attenuation.

2.4. Parameters setup of waveguide models used for the characterization of bounded periodic media

First, it is useful to get the dispersion curves for an infinite periodic medium in this 1D case using the F-B approach. The geometry parameters and the material properties of the unit cell defined in Table I are used. As the periodicity is only in the $\boldsymbol{e}_1$ direction and free edge conditions are applied on the horizontal boundaries, the Brillouin irreducible zone is reduced to a segment: $-X \rightarrow \Gamma \rightarrow X$ (Figure 5(left)). The dispersion curves are obtained from the numerical solution of the eigenvalue problem (3), for $\boldsymbol{k} = k\boldsymbol{e}_1$ with k evolving between $-\frac{\pi}{c}$ and $-\frac{\pi}{c}$. Figure 5(right) thus presents the eigenvalues $\omega(\boldsymbol{k})$ calculated numerically on the unit cell. For each value of the Bloch wave vector $\boldsymbol{k}$, the first six modes are calculated. It is noted the existence of frequency bands (in purple), for which there is no corresponding real wave vector $\boldsymbol{k}$. These are frequency bandgaps of the periodic medium. The first one appears around 300 Hz in particular.

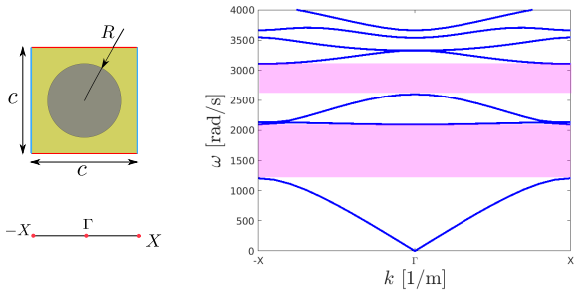

Figure 5: Unit cell Q_0 and associated Brillouin zone $Q^0 = -X \rightarrow \Gamma \rightarrow X$ (left) used to obtain the dispersion curves (right). The periodicity conditions are drawn in blue, and the edges in red are free edges.

Now, bounded periodic domains are considered, and it is expected that the presence of a finite number of periodically placed matrix-inclusion cells in the useful area (L_u) of the waveguide modifies the spectrum. Thus, to properly compare such a waveguide with the reference homogeneous waveguide, the parameters introduced previously must be chosen in an appropriate way. A key point here is to assess the effect of the marginal zone (L_m) on the obtained spectrum and characteristic modes of the waveguide.

To study the influence of L_u, (i.e., the size of the useful area) on the evolution of the valid frequency domain, an example is first studied with a single unit cell to observe the spectrum and characteristic modes of the

waveguide. For this example, the parameters are $L_u = c$, and $L_m = 0$m (Figure 6(a)). The parameters used for the geometry and properties are those of Table I. The eigenvalue solutions (ω) of the problem (Eq.(1)) for the waveguide are shown in the complex plane in the Figure 6, with the dispersion curves of the infinite periodic medium (*cf.* Figure 5) shown in red for comparison.

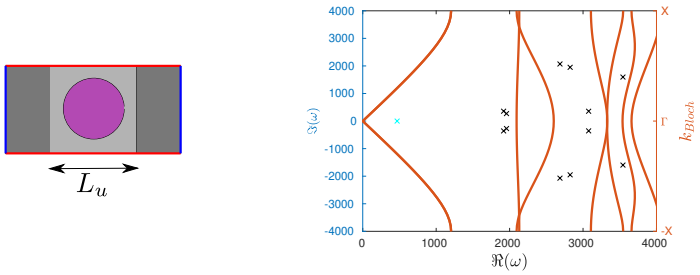

Figure 6: Study of a 1D waveguide model with $L_u = c = 1$ m and $L_m = 0$ m. (left) Model definition; (right) Eigenvalue solutions showing lack of information on the low-frequency propagative modes, and compared with the behaviour of the infinite periodic medium solved with F-B approach (presented in red).

According to the obtained results, a first problem appears: due to the very short length of the model, (i.e., L_u is very small), the modal analysis of the waveguide does not give enough information in the low-frequency domain. Thus, the density of available modes in $[0, 4500]$ rad/s the frequency range of interest is low compared to the homogeneous solution (Figure 3). Indeed, the longest wavelength taken into account by the waveguide model is of the same order of magnitude as L_u, which, in the current case, corresponds to the frequency of about 4000 rad/s. So the frequencies taken into account by this model are higher than the first two bandgaps considered here.

It is, therefore, necessary to increase $L_{tot} = 2 \cdot L_u$ the total length of the waveguide to reach the low-frequency range. For that, one of the solutions is to increase the length of the margins L_m between the PMLs and the bounded periodic medium so that L_u is close to the longest wavelength of interest. In the case of the waveguide with a single cell, this choice results in a value of L_m almost equal to the longest wavelength considered.

However, when the number of cells increases (n_{cells}), if it is chosen to keep L_m unchanged, the waveguide becomes longer and longer. This choice leads to obtaining many modes, which are not interesting because they evolve outside the bounded periodic medium and pollute the interpretation of the

results. It is, therefore, necessary to decrease L_m so that the size of the waveguide does not increase with the number of cells.

Other ways around this problem are out of scope for this paper but in summary, for the setup of the numerical waveguide model, the final solution adopted is to keep the length $L_{tot} = 2 \cdot L_u$ constant, large enough to analyze up to a large number of cells, while to adapt the length L_m according to the number of cells. Another advantage of such a setup is that the frequency domain in which all waveguides evolve (with different numbers of inclusions) is identical, so the comparison is easier. Thus in the following, it is proposed to use a waveguide of the same length, the one already defined for the study of the homogeneous waveguide in the previous section, whatever the considered number of cells.

Then the case of a single cell is studied again with this setup, and the obtained spectrum is represented in the Figure 7. As expected, the same essential spectrum, now represented by magenta dots, is obtained (Figure 3). Indeed, the existence of a single cell far away from the PMLs does not significantly disturb the essential spectrum. As the essential spectrum represents the behavior of the waves in the PMLs (i.e., at infinity), they are not taken into account in the following analysis of the attenuated frequency bands. It is rather the analysis of the other modes, associated with the discrete spectrum and concentrated around the real axis, will highlight the attenuation and the convergence to the bandgaps predicted by the F-B theory for the infinite periodic network.

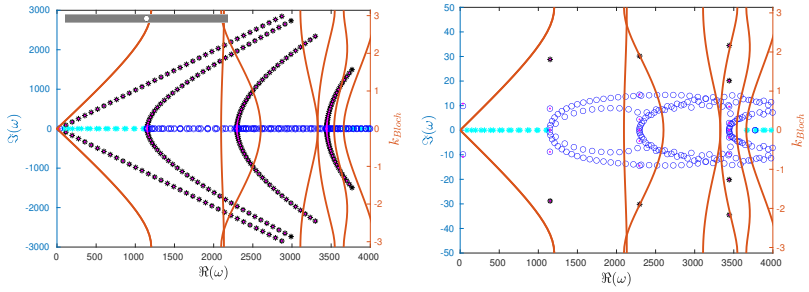

Figure 7: Spectrum (left) and its zoom around the real axis (right) of the studied waveguide with a single unit cell, compared with the dispersion curves (in red) of the corresponding infinite periodic medium obtained by F-B analysis.

Within the discrete spectrum, the modes associated with a complex eigenvalue with a nonzero imaginary part, displayed in blue or black in the Figure 7, are attenuated and show two types of behavior, illustrated in the

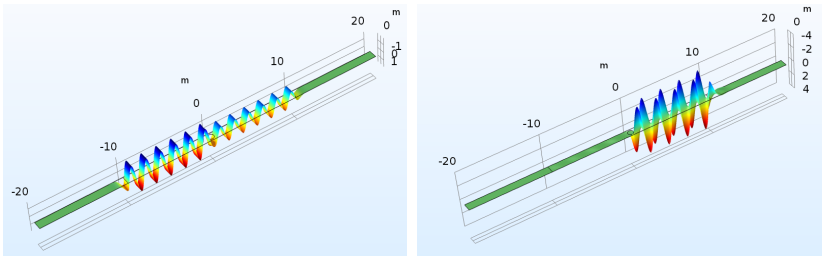

(a) (b)

Figure 8: Two types of modes in the discrete spectrum of a waveguide with a single inclusion. (a) Mode attenuated by the presence of an inclusion; (b) Mode reflected by the presence of the inclusion.

Figure 8. The discrimination between these two types of modes is set to a value of the imaginary part equal to 20 rad/s. This value corresponds to 95% attenuation of signal over a distance of $4c$. The Figure 8(a) presents a mode attenuated by the presence of the matrix-inclusion that still propagates in the medium (displayed in blue in the Figure 7). The eigenfrequency of this mode is $\omega = 1338 + 5.45i$ rad/s. The Figure 8(b) shows a mode not transmitted after the inclusion, as its eigenvalue has a rather large imaginary part (displayed in black in the Figure 7) The eigenfrequency corresponding to this mode is $\omega = 1497 + 10.5i$ rad/s. Such a mode can be considered as a mode reflected by the matrix-inclusion cell.

A comparison between the discrete spectrum and the dispersion curves of the infinite periodic medium shows that the study of a bounded medium with only one cell does not agree at all with the modeling of an infinite medium (Figure 7), which is quite normal. Indeed, only the first passband, between 0 and 1200 rad/s, is completely recovered by the real discrete eigenvalues. Otherwise, nearly all the other eigenvalues in σ_{disc} are complex numbers and do not give rise to well-distinguished bandgaps. Now the main idea is to use this waveguide model to determine the minimum number of matrix-inclusion cells needed to recover the bandgaps behavior of the infinite medium within the frequency range of interest considered.

In practice, the number of periodic matrix-inclusion cells is limited to a finite number. For instance, modifying soils in a dense urban area can be costly due to various constraints. It is thus of significant interest to evaluate with precision for a bounded periodic metamaterial the effectiveness of the analytically predicted frequency bandgaps using Floquet-Bloch theory

regarding their position and bandwidth.

3. Quantitative analysis of effective properties of bandgaps of 1D bounded periodic media

The parametric study using numerical models based on the above-mentioned principle is now presented. The influence of the number of periodically placed cells on the wave modes is analyzed. The results are compared with those of the corresponding infinite domain obtained by considering only the unit cell using the F-B transform.

3.1. Parametric study setup, analysis of discrete spectra, and characterization of modes

As explained in the previous section, in order to consider identical frequency ranges (i.e. corresponding to comparable wavelengths), the length of the waveguide L_u is determined by the largest number of cells considered in this study. Thus, with the choice of a periodic cell of side $c = 1$ m and a maximum number of eighteen inclusions, the useful zone is chosen of length $L_u = 20$ m. The length of each PML is chosen to equal half the total length of the useful area L_u, $L_{PML} = 10$ m, in all models in order to limit the number of modes of the essential spectrum calculated. A consequence of keeping the waveguide length constant is that the size of the margins varies according to the number of cells to be considered. The material properties and parameters of the elementary cells are defined in Table I.

In the following, the modal analysis of the waveguide, including a bounded periodic medium and, in particular, its discrete spectrum, is compared to the dispersion curves obtained theoretically for the corresponding infinite periodic medium (Figure 5). The results for four values of the number of cells, 3, 9, 15, and 18, are presented in Figure 9.

As for the 1-cell case (Figure 7), the computed eigenvalues are represented in the complex plane: the real eigenvalues are shown in cyan, the complex ones with an imaginary part less than 20 rad/s in blue, and the other complex ones in black. The essential spectrum of the model without inclusions is represented by magenta dots. Systematically, the figures on the right are enlargements of those on the left of the area around the axis of the reals, and so, in particular, they do not display most of the modes of the essential spectrum. The dispersion curves predicted by the F-B theory of the corresponding infinite periodic medium are plotted here in red.

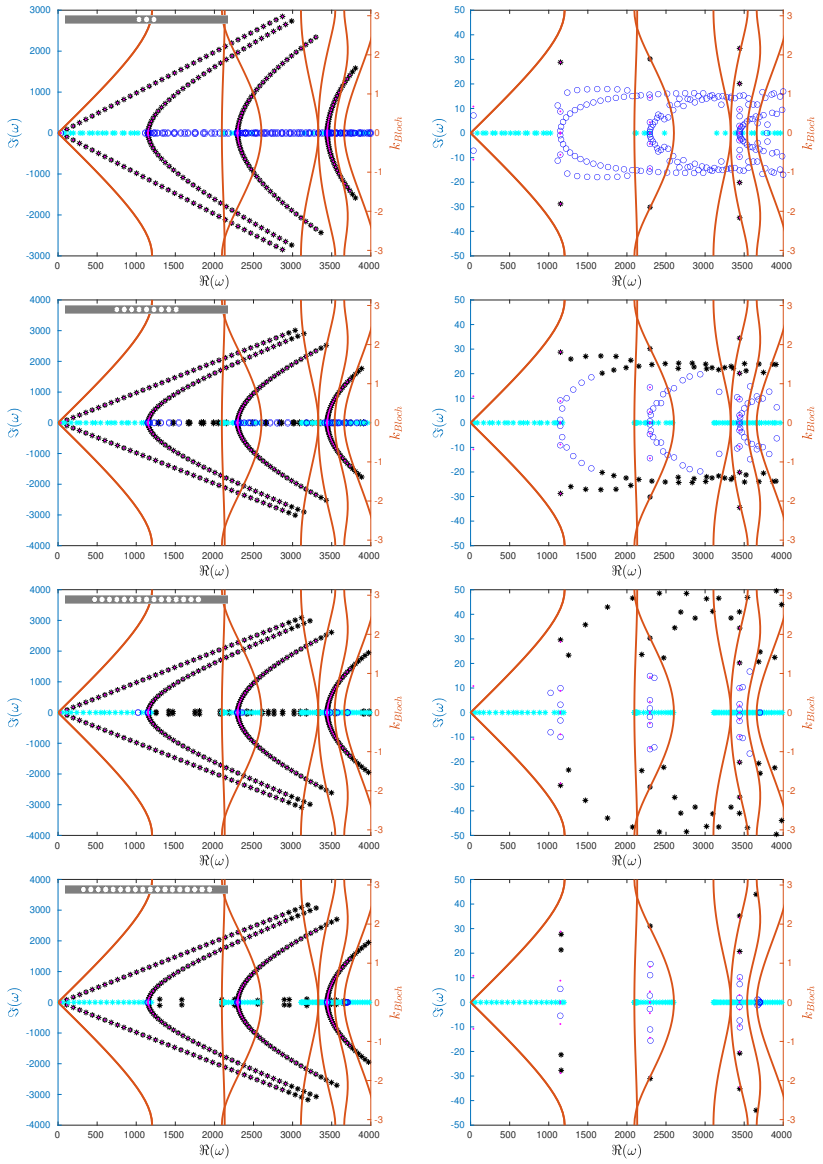

Figure 9: Parametric study on the influence of the number of cells on the eigenvalue spectrum and comparison with the dispersion curves (in red) obtained with the F-B theory for the corresponding infinite periodic medium. Spectrum (left) and its zoom around the real axis (right) of the studied waveguides with 3, 9, 15, and 18 unit cells. The real eigenvalues of the discrete spectrum are displayed in cyan. The complex eigenvalues with an imaginary part smaller than 20 rad/s are displayed in blue, and the others in black. The essential spectrum of the model without inclusions is displayed with magenta dots.

Again from Figure 9, as expected, the larger the number of cells, the fewer the modes with real eigenvalues (cyan) or complex eigenvalues with a small imaginary part (blue) in the frequency bandgaps predicted by the F-B theory. The modes associated with a complex eigenvalue that remain in the bandgaps are either a reflected mode concentrated in the margins between the PML and the edge of the bounded periodic medium (Figure 8(b)) or a mode with a decreasing amplitude into the periodic media like the one displayed on the Figure 10. Identifying the type between both of these modes cannot be done without analyzing their shapes.

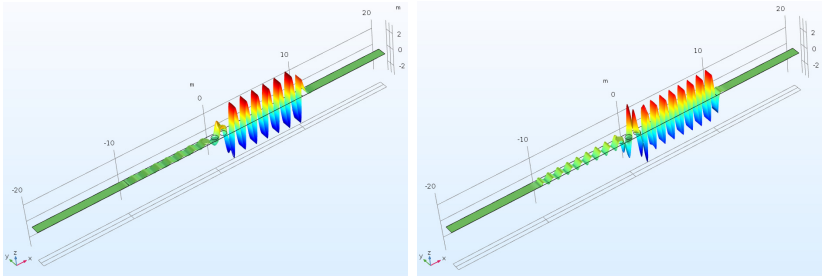

Figure 10: Mode attenuated into the periodic media (case with 3 inclusions). The imaginary part is equal to 17.9 rad/s (left) and to 15.1 rad/s (right).

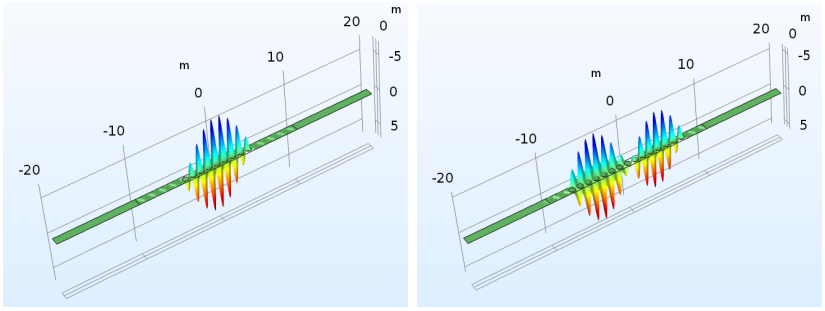

Figure 11: Trapped modes in bounded periodic media with respectively (left) 9 and (right) 15 inclusions.

Moreover, the imaginary parts of the complex modes of the discrete spectrum increase with the number of cells. Thus, the type of modes that are only attenuated but still able to propagate to the other side of the bounded periodic medium, observed in the case with a small number of cells (Figure 8 (a)), is less present in the case with a larger number of cells. For instance, in the case of five cells, such modes are no longer visible among the calculated ones. Thus, the complex modes of the discrete spectrum within the

bandgaps are all like the modes shown in (Figure 8(b)) and in Figure 10, i.e.,"*stopped*" or "*reflected*" by the bounded periodic medium. Hence, the waveguide's behavior approaches that of an infinite medium in terms of band gaps when the number of inclusions increases. For the two modes shown in Figure 10, the values of the eigenfrequencies are $\omega = 1749 + 17.9i$ rad/s and $\omega = 2128 + 15.1i$ rad/s.

Furthermore, the increase in the number of cells also makes it possible to observe the appearance of trapped modes in the bounded periodic medium. Two examples in the cases with respectively nine and fifteen cells are given in Figure 11. These modes are trapped in the bounded periodic medium; in other words, they are propagative modes in the corresponding infinite periodic medium. The corresponding eigenfrequencies are $\omega = 2096$ rad/s (9 cells) and $\omega = 2097$ rad/s (15 cells). In the spectrum, the eigenvalues of these trapped modes are always real, whatever the model of PML used in the numerical model, conjugate or classical. Hence, the analysis of the spectrum obtained with the classical PMLs makes it possible to differentiate them from the propagative modes obtained outside frequency bandgaps because these bandgaps are associated with complex eigenvalues. The Figure 12 presents the spectrum obtained for the case with nine cells using the model with the classical PMLs. Thanks to this change in the definition of the PML, some trapped modes (cyan) are distinguished close to the border of frequency bandgaps (especially several modes that appear around 2100 rad/s). However, it is no longer possible with this definition to distinguish the propagative modes outside the frequency bandgaps from the attenuated and reflected modes by the periodic medium. In other words, using conjugate PLMs in these models highlights the complex modes that are interesting because they are in the forbidden frequency bands.

3.2. Convergence and effectiveness analysis: Number of cells necessary to validate the periodicity hypothesis

The Figure 13(left) summarizes the previous results by representing only the real modes as a function of the number of inclusions. The curve corresponding to the infinite case shows the dispersion curves obtained using the F-B transform, the red curves shown in any previous spectrum figure and projected onto the horizontal line when the k_{Bloch}-axis is compressed to one point. It should be noted that when the number of cells is small, the large frequency bands with no real modes cannot be "identified" as a frequency

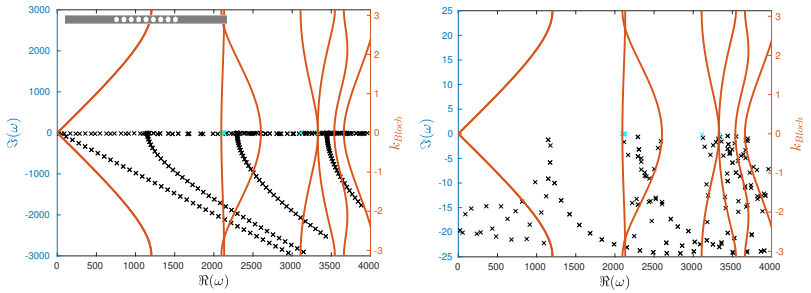

Figure 12: Spectrum obtained with non-conjugated PMLs (left) and a zoom (right) around the real axis to highlight the trapped modes for the case of 9 inclusions.

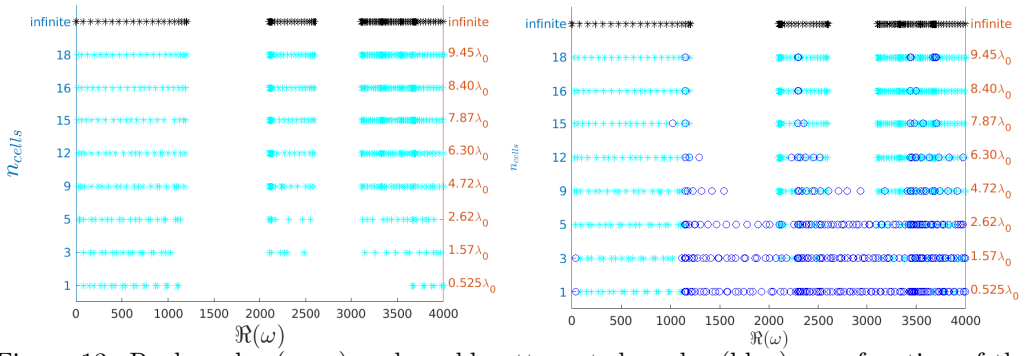

Figure 13: Real modes (cyan) and weakly attenuated modes (blue) as a function of the number of cells with (left) real modes only and (right) real and weakly attenuated modes

bandgap. Indeed, it will show that complex modes with a small attenuation coefficient (the imaginary part of the eigenvalue) exist in these bands (Figure 13(right)).

In Figure 13(left), the y-axis on the right shows the equivalence of the size of the periodic medium in terms of wavelength. The chosen reference wavelength, $\lambda_0 = 0.525$ m, corresponds to the wave propagating in the matrix at the lowest frequency of the first frequency bandgap of the infinite periodic medium, which is $\omega_0 = 1204$rad/s.

For the numerical models considered here, two frequency bands are predicted in the infinite case. For the i-th bandgap ($i = 1, 2$), its position is defined by ω_i^{inf} the frequency at its middle and W_i^{inf} its width (*cf.* Figure 5). Then the values obtained numerically on a bounded medium, ω_i and W_i, are compared to these reference values $(\omega_i^{inf}, W_i^{inf})$ by using two

"effectiveness" indicators I_ω and I_W defined as follows:

$$I_\omega = \frac{1}{N}\sum_{i=1}^{N}\epsilon_{\omega_i}, \text{ with } \epsilon_{\omega_i} = \frac{|\omega_i - \omega_i^{inf}|}{\omega_i^{inf}} \tag{10a}$$

$$I_W = \frac{1}{N}\sum_{i=1}^{N}\epsilon_{W_i}, \text{ with } \epsilon_{W_i} = \frac{|W_i - W_i^{inf}|}{W_i^{inf}} \tag{10b}$$

The evolution of these effectiveness indicators as a function of the number of cells, by counting only the real modes, is given in the Figure 14. For these examples, $N = 2$. Thus, it could be concluded that when the size of the bounded periodic medium is greater than four times the reference wavelength, i.e., containing about nine cells, its behavior regarding the first two frequency bandgaps begins to reach that of the infinite medium. In other words, the effectiveness in terms of bandgaps predicted for the infinite medium is almost recovered by such a bounded medium. These results are in agreement with previous works [20, 30, 31, among others].

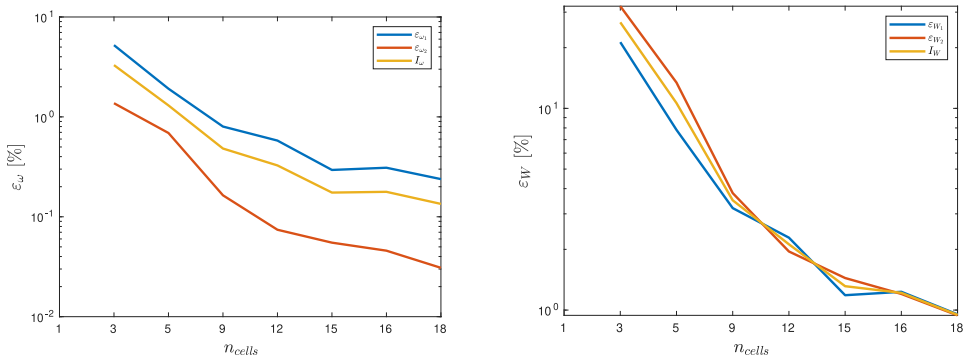

Figure 14: Evolution of the effectiveness indicators on (left) the position (average frequency) and (right) the width of frequency bandgaps by counting the real modes alone.

As already indicated, the previous analysis is not appropriate when the bounded domain contains only very few cells because the observed large frequency bands with no real mode cannot be considered as a frequency bandgap. Therefore, an improved approach is proposed below to perform a more qualitative analysis of effectiveness for bounded periodic media.

The idea consists of considering the complex modes with an imaginary part lower than a certain threshold in addition to the real ones. The Figure 13(right) shows the real modes and the complex modes with an imaginary

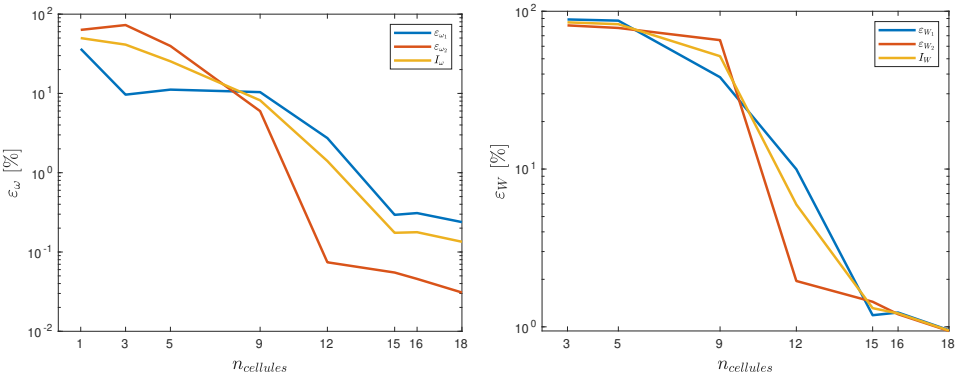

Figure 15: Evolution of the effectiveness indicator on (left) the average frequency and (right) the width of frequency bandgaps by counting real modes and weakly attenuated modes.

part smaller than 20 rad/s (displayed in blue); the latter lets part of the wave propagate through the bounded periodic medium. It can be seen that this analysis is more relevant because large frequency bands without modes are no longer observed in cases with very few cells. Hence, it allows us to better compare the effectiveness of bounded periodic media to the infinite one by taking into account the weakly attenuated modes.

Concerning the calculation of the effectiveness indicators, the width W_i is obtained by looking for the maximum difference between two successive weakly attenuated modes, the blue points, and the identified interval also gives the average frequency ω_i.

The evolution of the effectiveness indicators by counting both real and weakly attenuated complex modes as a function of the number of cells is given on the Figure 15. It highlights the fact that it converges to the values obtained for the infinite medium when the number of cells increases. The indicators on the average position (ε_{ω_i} and I_ω) are smaller than the ones on the width (ε_{W_i} and I_W) of the bandgaps. Thus, from twelve cells, the indicator on the position is lower than 5% while that on the width is around 15%. For the position, the indicator goes down to 0.2% for fifteen cells if we consider each band separately, and the indicator on the width is lower than 2% for this number of cells.

4. Quantitative analysis of effective properties of bandgaps of 2D bounded periodic media

The waveguide modal analysis presented above allows the study of bounded periodic media only in the $\mathbf{e}_1$ direction but not the consideration of 2D periodicity. In order to analyze 2D-periodic barriers, infinite in the $\mathbf{e}_2$ direction and bounded in the $\mathbf{e}_1$ direction, it is possible nevertheless to prescribe the F-B conditions on the horizontal boundaries, which were assumed to be free of stresses in the previous modeling (Figure 5). Thus, the previously implemented waveguide models are extended to 2D-periodic media by adding a second direction of periodicity along $\mathbf{e}_2$. By adding periodicity conditions on the horizontal boundaries, the new waveguide models contain infinite cells in the $\mathbf{e}_2$ direction while remaining with a finite number of cells in the e_1 direction. The Figure 16 presents the problem thus defined.

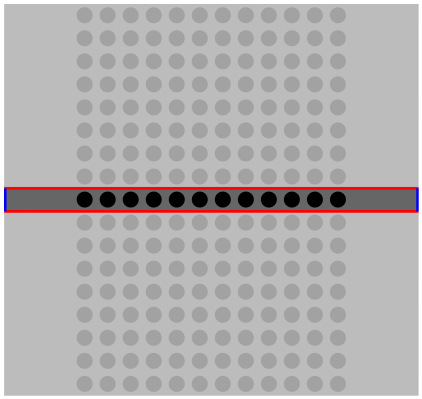

Figure 16: 2D-periodic barrier and its waveguide model with a single row of cells shown in dark gray (with inclusions in black), which is the elementary cell used for the F-B transform Equation (11) and the periodicity conditions are applied on its horizontal boundaries (red lines).

In this framework, the behavior of the waveguide is then governed by the following F-B equation:

$$(\nabla_{\mathbf{x}} + i\mathbf{k}) \cdot (\mu\,(\nabla_{\mathbf{x}} + i\mathbf{k})\,u) = -\rho\omega^2 u. \tag{11}$$

with $\boldsymbol{k} = k_2\mathbf{e}_2$.

For the new waveguide models, the definition of the PMLs remains unchanged (see Eq.(9)) because it is not affected by the F-B transform and the change of variable in the PMLs is only on the x_1 variable.

In the following, the results obtained with the waveguide models are analyzed and compared with the frequency bandgaps of the corresponding infinite 2D-periodic medium, predicted by the F-B theory (Figure 17(c)). In this Figure, the Bloch wave number is presented in abscissa following the contour of the Brillouin irreducible zone $M \rightarrow \Gamma \rightarrow X \rightarrow M$. In the same way as before, the dispersion curves are obtained from the numerical solution of the eigenvalue problem (Eq.(3)). It is remarked that, compared to the 1D periodic case (Figure 5), the first two bandgaps are narrower and move towards the higher frequency range.

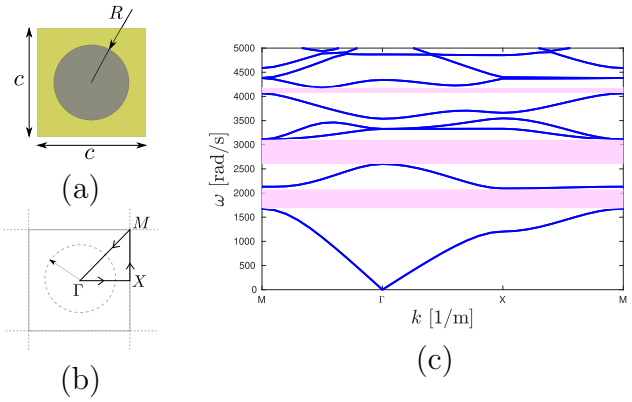

Figure 17: Unit cell Q_0 of the periodic medium in physical space and corresponding first Brillouin zone Q^0 in reciprocal space. (a) A unit cell corresponding to an infinite medium in two directions; (b) A reciprocal cell on which the contour of the Brillouin irreducible zone, $\Gamma \rightarrow X \rightarrow M \rightarrow \Gamma$, is represented; (c) Dispersion curves highlighting bandgaps.

4.1. Analysis of discrete spectra, characterization of modes, and ability to reconstruct the 2D periodicity behavior

Following the proposed approach, the combined waveguide and F-B modal analysis are performed for the set of k values sweeping the entire Brillouin zone $\left[\frac{-\pi}{c}\frac{-\pi}{c}\right]$ in the $\mathbf{e}_y$ direction in which the F-B conditions are applied. The obtained modes are then plotted to show the spectrum of each F-B waveguide.

First, as presented previously for the case of 1D propagation, Figure 18 shows the spectrum of a homogeneous waveguide without any inclusion. It can be seen that, compared to the previous 1D-periodic case, many more modes are obtained for the essential (black) and discrete (cyan) spectra. Indeed, each value of k in the Brillouin zone gives rise to a different spectrum.

Thus, the modes obtained should be more complex to analyse than in the 1D case.

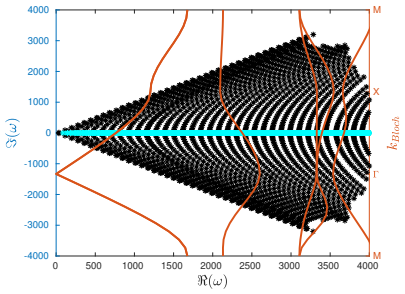

Figure 18: Spectrum of the homogeneous waveguide in the complex plane: σ_{disc} with real eigenvalues (cyan) and σ_{ess} (black); Dispersion curves (in red) obtained with the F-B theory.

Moreover, contrary to the essential spectrum obtained in the 1D-periodic case (Figure 3), many modes belonging to the essential spectrum are very close to the real axis. Therefore, it would not be easy to distinguish them from the complex modes belonging to the discrete spectrum of waveguide models with inclusions.

A parametric study on the number of cells similar to that carried out previously for the 1D case is set up. The number of cells ranges from one to eighteen cells. The spectrum results are given in Figure 19. It is noted immediately that the frequency bands defined by the real modes (in cyan) of the waveguide models coincide with the passbands defined by the propagating modes of the corresponding 2D infinite medium calculated with the F-B transform (in red). Therefore, it can be concluded that our waveguide models that consider only one of the infinite directions can be used to gradually approach the bandgap solution of the corresponding 2D infinite periodic medium.

As for the previously presented 1D-periodic waveguide models, the density of real modes increases with the number of cells within theoretically predicted passbands.

Inside the theoretically predicted bandgaps, as before, there are non-real modes, and their number depends on the number of cells. They are attenuated modes (since they have a non-zero imaginary part). However, unlike the periodic 1D case, some complex modes close to the real axis always appear, i.e., with a relatively small imaginary part, even when the number of cells increases. This is due to the periodicity in the $\mathbf{e}_2$ direction conserved

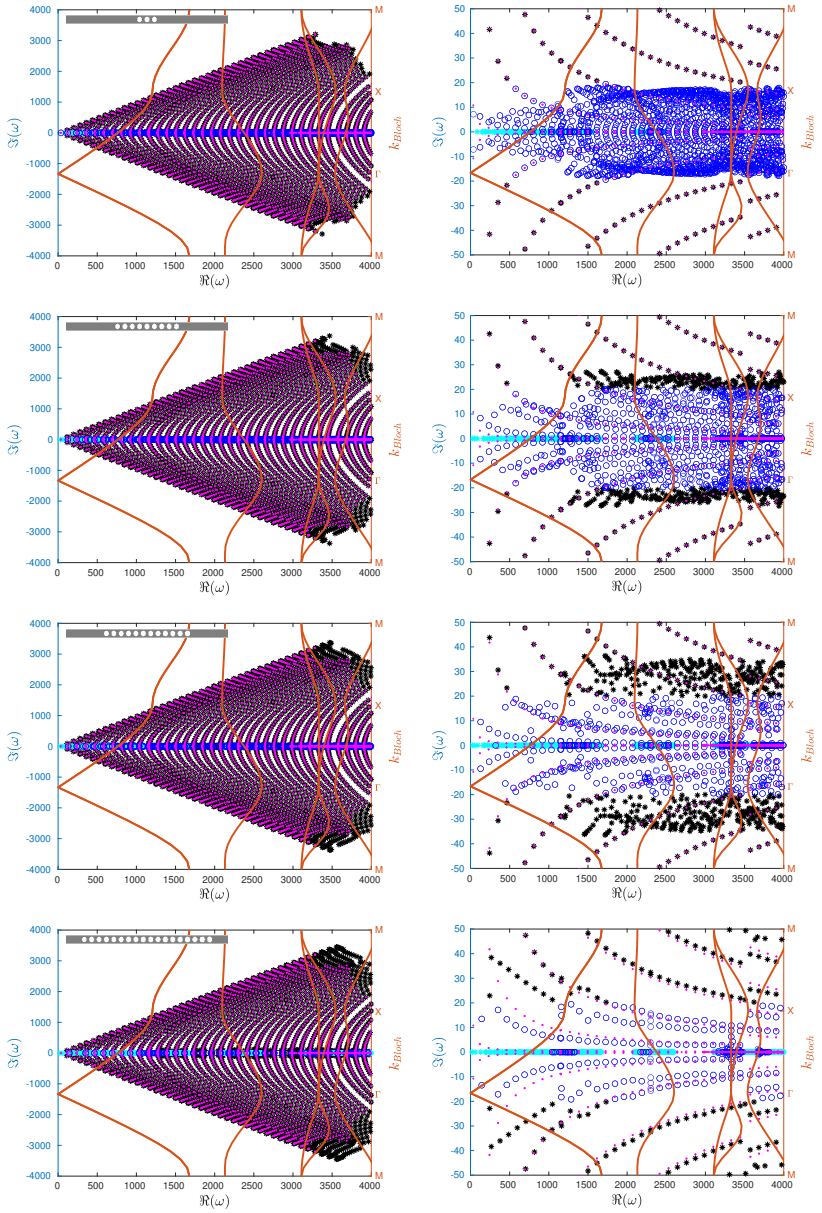

Figure 19: Parametric study on the influence of the number of cells on the eigenvalue spectrum and comparisons with the dispersion curves (in red) obtained with the F-B theory for the corresponding infinite 2D periodic medium. Spectrum (left) and its zoom around the real axis (right) of the studied waveguides with respectively 3, 9, 12, and 18 cells. The real eigenvalues of the discrete spectrum are in cyan. The complex eigenvalues with an imaginary part smaller than 20 rad/s are in blue, and the others are in black. The essential spectrum without inclusions is displayed with magenta dots.

in our F-B waveguide models. An example of such a mode is given in Figure 20(left). The real part of its eigenvalue is 1828.3 rad/s, and the imaginary part is equal to 15.2 rad/s for a value of k equal to 1.57. It is a mode of the essential spectrum. The behavior of this mode looks like a reflected mode despite its low imaginary part. Because of the periodicity in the e_2 direction, and so the fact that the wave also propagates in the transverse direction e_2, this mode is weakly influenced by the periodic medium's size. Hence, it is a mode propagating in the direction e_2 and localized in the margins between the bounded periodic medium and the PML. As the size of the margins decreases when the number of cells increases, these modes move away from the real axis, but not as quickly as the other complex modes, "stopped" or attenuated by the bounded periodic medium. Note that the thinner the margins, the more the essential spectrum is modified compared to the one of the homogeneous waveguide (represented by the pink points). However, it keeps the same smooth shape.

To compare, Figure 20(right) represents a complex mode of the model with nine cells obtained for $k = 2.51$ m^{-1}, for which the imaginary part of its eigenvalue is equal to about 23 rad/s and a real part equal to 1903 rad/s. In this case, the wavefront propagates along the e_1 direction and is attenuated by the bounded periodic medium. This type of mode rapidly moves away from the real axis when the number of cells increases. It can be seen that, for waveguide models with a large number of cells, the only modes that stay close to the real axis in the theoretically predicted frequency bandgaps are those from the essential spectrum.

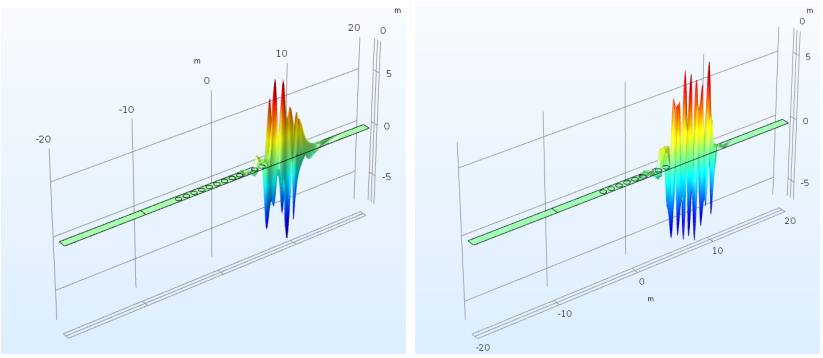

Figure 20: (left) Propagative mode in the direction e_2 (case of 12 inclusions) and explaining the modes inside the bandgaps; (right) Attenuated mode in the direction e_1 (case of 9 inclusions).

4.2. Convergence and effectiveness analysis: Number of cells necessary to validate the periodicity hypothesis

As in the 1D analysis, Figure 21 displays the real modes as a function of the number of cells. The conclusions previously made for the 1D periodic waveguide models apply. For a small number of cells, the density of real modes is very low, which does not mean that large frequency bandgaps are obtained. When the number of cells increases, the analysis becomes relevant; thus a convergence study on the effectiveness of the considered bounded periodic media could be carried out.

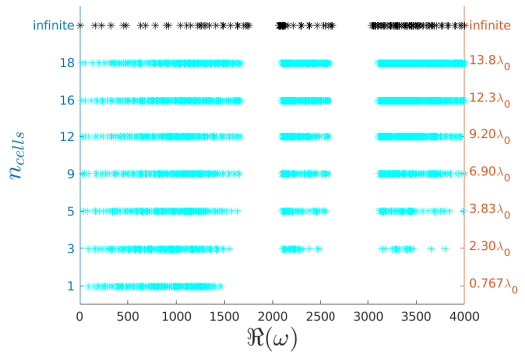

Figure 21: Real modes versus the number of inclusions (2D model).

In the same way as before, Figure 22 presents the evolution of the effectiveness indicators given by the equations (10a) and (10b) as a function of the number of cells. For the model with only one cell, the indicators are not computed for the obvious reason that only one large "attenuated" frequency band, instead of two, is obtained in the ω interval considered. These figures show the decrease of the error committed by adding inclusions in the $\boldsymbol{e}_1$ direction. It is important to remark that the effectiveness indicators are better regarding the position of the frequency bandgaps (less than 5% from three cells in the $\boldsymbol{e}_1$ direction) than their width.

It is also noted that the evolution of effectiveness indicators by counting the real and weakly attenuated complex modes like that done for the 1D periodic waveguide models is not presented here. Indeed, it is more complicated to distinguish the weakly attenuated complex modes from the complex modes of the essential spectrum, as already explained above. Indeed, the removal of the modes of the essential spectrum close to the real axis to take into account only the other complex modes linked to the useful zone (the

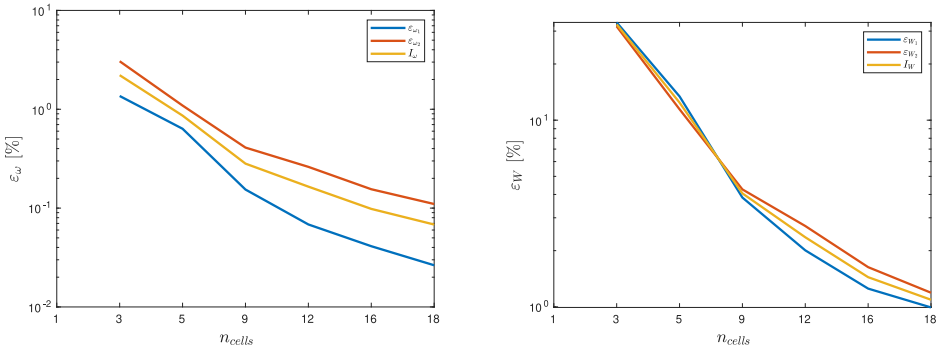

Figure 22: Evolution of the effectiveness indicators on (left) the position (average frequency) and (right) the width of frequency bandgaps, by counting the real modes alone.

bounded periodic medium), i.e., those of the discrete spectrum, is for the moment possible but at the price of manual sorting, which is laborious. Nevertheless, such a study is possible if more quantitative characterization is required with the development of more automatic tools.

5. Application to locally resonant metamaterials

In this section, the previously proposed method is applied to analyze a bounded 1D- and 2D-periodic matrix-inclusion medium with local resonators or resonant metabarriers.

In order to obtain frequency bandgaps at lower frequencies while keeping a reasonably small size of the periodic cells, as it is expected for seismic purposes, one of the main solutions is to use locally resonant metamaterials [9, 12, 17, 43, 47, 48, among others]. The local resonator conception chosen for this study was proposed in Liu et al.'s work [43] by using Helmholtz resonators made by a heavy mass inside a very soft intermediate layer (Figure 23(a)). The dimensions and the materials properties for the soft intermediate layer (μ_s, ρ_s) and for the heavy mass inside (μ_i, ρ_i) are given in Table II, the materials properties for the matrix (μ_m, ρ_m) being unchanged and already given in Table I.

As in the previous cases, the dispersion curves for the infinite medium are obtained by applying the F-B theory to an FE model of the unit cell. They are represented in Figure 23(b) for the 1D-periodic model and in Figure 23(c) for the 2D-periodic one. It is important to note that, for the same cell size, the first frequency bandgap appears in a very low-frequency range, around

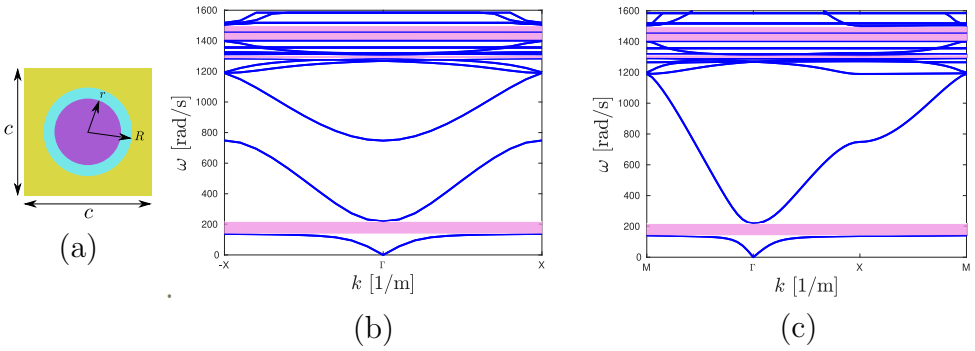

Figure 23: Locally resonant material made of Helmholtz resonator. (a) Unit cell (left), dispersion curves obtained by the F-B theory in the infinite case (b) with 1D-periodicity and (c) 2D-periodicity.

c (m)	R (m)	r (m)	μ_s (GPa)	μ_i (GPa)	ρ_s (kg/m^3)	ρ_i (kg/m^3)
1	0.346	0.260	0.0015	210	1200	7850

Table II: Summary of the data used for the simulation of the 2D-periodic medium with local resonators, where subscripts "s" and "i" represent the intermediate soft layer and the central heavy mass, respectively.

200 rad/s, instead of 2000 rad/s in the case considered in the previous sections (i.e. without local resonators).

A parametric study is performed by modifying, as previously, the number of cells, going from three to eighteen cells, in the waveguide. The results of the 1D-periodic case are presented in Figure 24. As in the heretofore studied case, the real modes do not appear in the theoretically predicted bandgaps for the infinite reference case and some attenuated modes exist inside those bandgaps for the smaller number of cells. However, it is important to note that there are less attenuated modes than in the case of Bragg scattering models.

The Figure 25 summarizes the analysis of bandgaps by representing only the real modes and weakly attenuated modes as a function of the number of cells, and the same conclusions as for the Bragg scattering are obtained. The higher the number of cells, the higher the effectiveness of the waveguide with periodic media, and also it could be considered that the first frequency bandgap predicted for the infinite case is recovered with 18 cells.

As the frequency of the first bandgap appears at a much lower frequency range, the density of points used to characterize the effectiveness of such

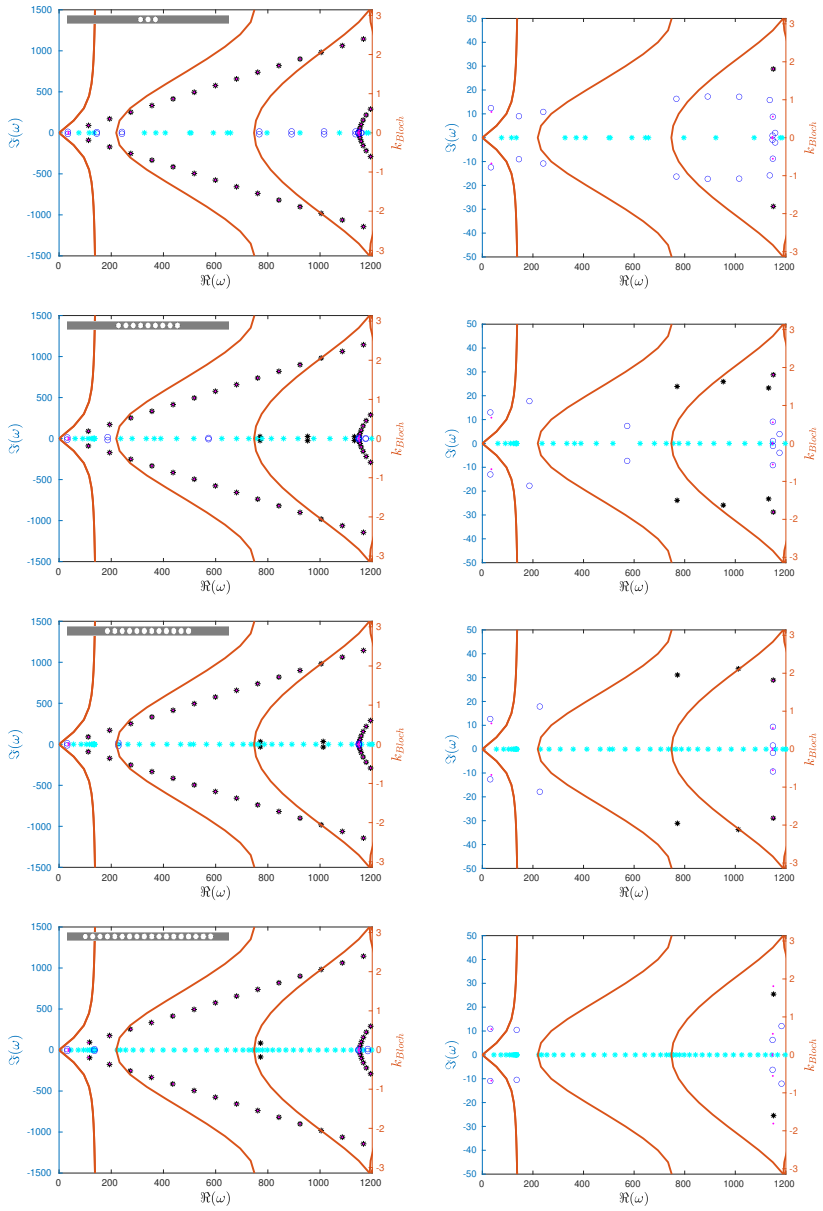

Figure 24: Parametric study on the influence of the number of cells on the eigenvalue spectrum and comparisons with the dispersion curves (in red) obtained with the F-B theory for the corresponding infinite 1D-periodic medium. Spectrum (left) and its zoom around the real axis (right) of the studied waveguides with respectively 3, 9, 12, and 18 cells. The real eigenvalues of the discrete spectrum are in cyan. The complex eigenvalues with an imaginary part smaller than 20rad/s are in blue, and the others in black. The essential spectrum without inclusions is displayed with magenta dots.

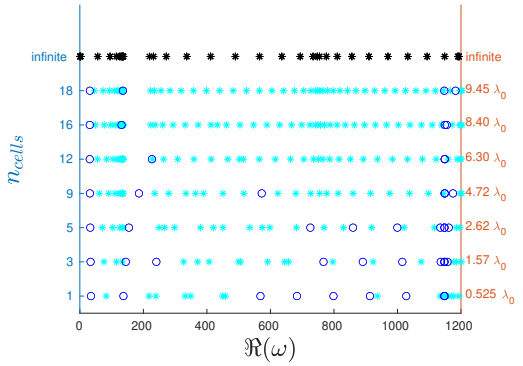

Figure 25: Real modes (cyan) and weakly attenuated modes (blue) as a function of the number of cells.

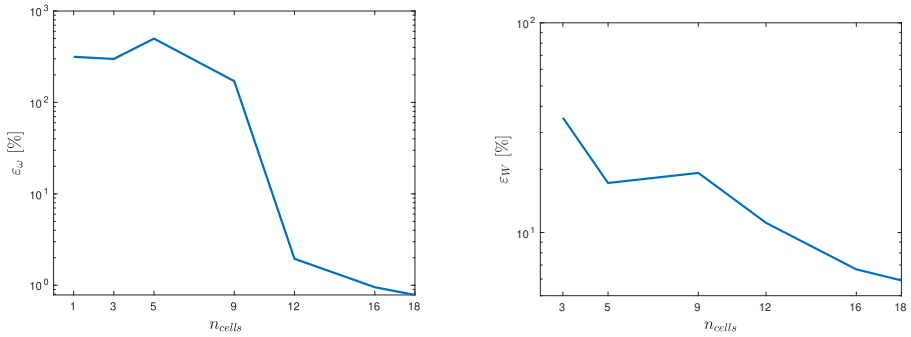

Figure 26: Evolution of the effectiveness indicator on (left) the average frequency and (right) the width of frequency bandgaps by counting real modes and weakly attenuated modes.

a bounded periodic media decreases. It would be useful to take a longer waveguide. However the same trend as in the Bragg scattering is visible: the more cells, the smaller the difference between infinite and finite cases. Thus, efficiency indicators are plotted on Figure 26 for the unique bandgap visible around 200 rad/s. It appears that the central frequencies are well evaluated for a number of cells greater than 12. The indicator is there around 2% and it is remarked that the effectiveness of the width of the bandgap also follows the same trend. The indicator only goes down to 10% for the highest number of cells (i.e. 18 cells).

As in the Section 4, the model 1D-periodic is then studied with a 2D-periodicity by applying F-B conditions on the horizontal boundaries of the

model. The spectrum of this model is shown on Figure 27 for a different number of unit cells. The red curves represent the 2D-periodic dispersion curves (Figure 23(c)). These results allow to recover the same behaviour as in the previous studies. The weakly attenuated modes inside the frequency bandgap disappear when the number of unit cells increases. Nevertheless, this tool (especially the way the modes are sorted) must be improved in order to have a way to quantify the effectiveness in the case of 2D-periodicity.

6. Conclusions

In this article, a method to quantitatively characterize the behaviours regarding acoustic waves of bounded 1D- and 2D-periodic metamaterials made with a matrix and circular inclusions have been presented. This approach allows a complementary analysis to the classical Floquet-Bloch approach dedicated to infinite periodic media. The proposed method is based on waveguide modal analysis. By using PML, it is possible to isolate the effects of the bounded metamaterial without dealing with boundary conditions. Two different types of metabarriers (i.e. with and without local resonators) were numerically analysed so as to assess the induced wave amplitude attenuation.

The findings reveal that a minimum number of cells is necessary to fit the theoretically predicted bandgaps obtained with the Floquet-Bloch theory. This minimum number of cells depends on the criteria defined in terms of wave attenuation by the bounded periodic medium. The waveguide modal analysis confirm that depending on the size of the bounded periodic medium, more or less attenuated complex modes can exist in the frequency bandgaps theoretically predicted.

Finally, the obtained results also indicate that in the locally resonant systems the first frequency bandgap appears in a very low-frequency range compared to the same configuration but without local resonators.

Acknowledgments

This work was granted by a Ph.D. scholarship from the École normale supérieure de Cachan/Paris-Saclay (CDSN).

CRediT authorship contribution statement

Michaël Darche: Conceptualization, Methodology, Software, Validation, Formal analysis, Writing - Original Draft, Writing - Review & Editing,

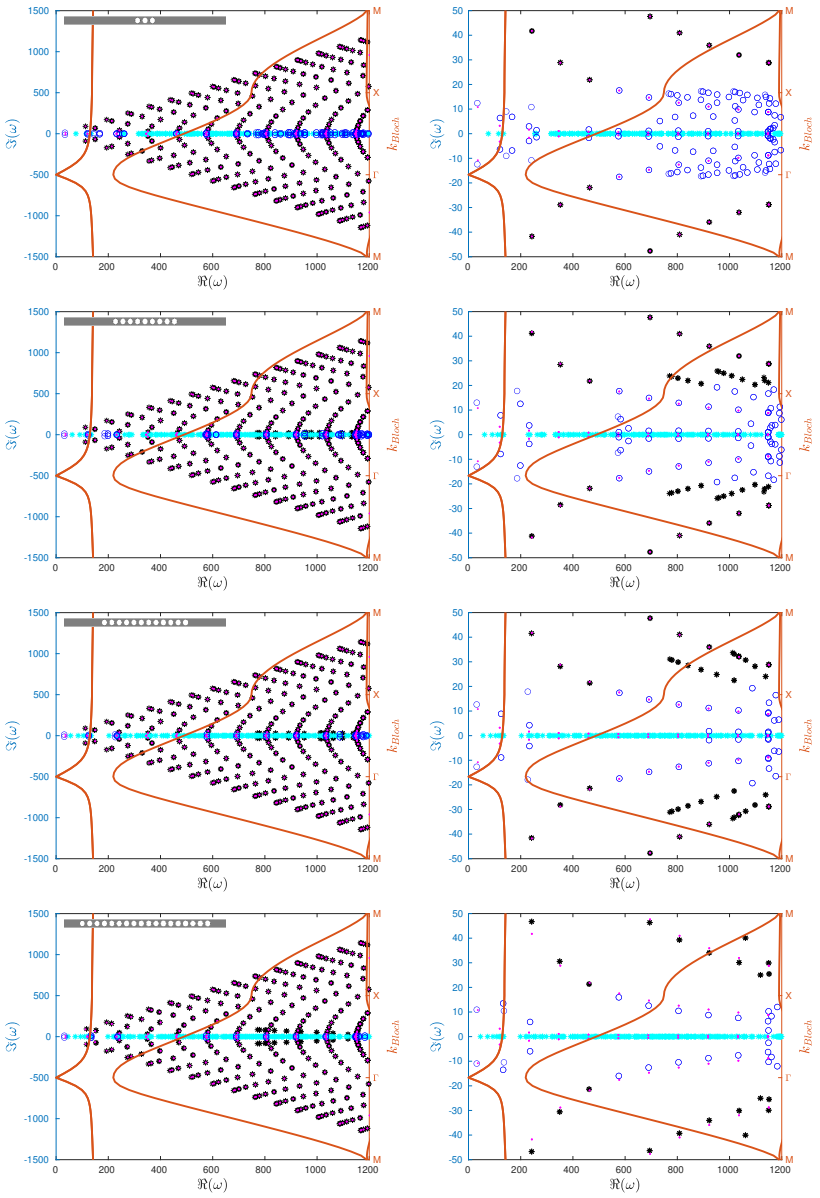

Figure 27: Parametric study on the influence of the number of cells on the eigenvalue spectrum and comparisons with the dispersion curves (in red) obtained with the F-B theory for the corresponding infinite 2D periodic medium. Spectrum (left) and its zoom around the real axis (right) of the studied waveguides with respectively 3, 9, 12, and 18 cells. The real eigenvalues of the discrete spectrum are in cyan. The complex eigenvalues with an imaginary part smaller than 20rad/s are in blue, and the others in black. The essential spectrum without inclusions is displayed with magenta dots.

Visualization. **Fernando Lopez-Caballero:** Conceptualization, Methodology, Formal analysis, Writing - Review & Editing, Visualization, Supervision, Funding acquisition. **Bing Tie:** Conceptualization, Methodology, Formal analysis, Writing - Original Draft, Writing - Review & Editing, Visualization, Supervision.

References

[1] S. Liao, D. A. Sangrey, Use of piles as isolation barriers, Journal of the Geotechnical Engineering Division 104 (1978) 1139–1152. doi:10.1061/AJGEB6.0000684.

[2] D. E. Beskos, B. Dasgupta, I. G. Vardoulakis, Vibration isolation using open or filled trenches, Computational Mechanics 1 (1986) 43–63. doi:10.1007/bf00298637.

[3] P. Tsai, Z. Feng, T. Jen, Three-dimensional analysis of the screening effectiveness of hollow pile barriers for foundation-induced vertical vibration, Computers and Geotechnics 35 (2008) 489–499. doi:10.1016/j.compgeo.2007.05.010.

[4] C. Murillo, L. Thorel, B. Caicedo, Ground vibration isolation with geofoam barriers: Centrifuge modeling, Geotextiles and Geomembranes 27 (2009) 423–434. doi:10.1016/j.geotexmem.2009.03.006.

[5] D. Ulgen, O. Toygar, Screening effectiveness of open and in-filled wave barriers: A full-scale experimental study, Construction and Building Materials 86 (2015) 12–20. doi:10.1016/j.conbuildmat.2015.03.098.

[6] S. Krödel, N. Thomé, C. Daraio, Wide band-gap seismic metastructures, Extreme Mechanics Letters 4 (2015) 111–117. doi:10.1016/j.eml.2015.05.004.

[7] Y. Achaoui, B. Ungureanu, S. Enoch, S. Brûlé, S. Guenneau, Seismic waves damping with arrays of inertial resonators, Extreme Mechanics Letters 8 (2016) 30–37. doi:10.1016/j.eml.2016.02.004.

[8] V. K. Dertimanis, I. A. Antoniadis, E. N. Chatzi, Feasibility analysis on the attenuation of strong ground motions using finite periodic lattices of mass-in-mass barriers, Journal of Engineering Mechanics 142 (2016). doi:10.1061/(asce)em.1943-7889.0001120.

[9] F. Basone, M. Wenzel, O. S. Bursi, M. Fossetti, Finite locally resonant metafoundations for the seismic protection of fuel storage tanks, Earthquake Engineering & Structural Dynamics 48 (2019) 232–252. doi:10.1002/eqe.3134.

[10] F. Zeighami, A. Palermo, A. Marzani, Rayleigh waves in locally resonant metamaterials, International Journal of Mechanical Sciences 195 (2021) 106250. doi:10.1016/j.ijmecsci.2020.106250.

[11] X. Wang, S. Wan, Y. Nian, P. Zhou, Y. Zhu, Periodic in-filled pipes embedded in semi-infinite space as seismic metamaterials for filtering ultra-low-frequency surface waves, Construction and Building Materials 313 (2021) 125498. doi:10.1016/j.conbuildmat.2021.125498.

[12] C. Kanellopoulos, N. Psycharis, H. Yang, B. Jeremić, I. Anastasopoulos, B. Stojadinović, Seismic resonant metamaterials for the protection of an elastic-plastic SDOF system against vertically propagating seismic shear waves (SH) in nonlinear soil, Soil Dynamics and Earthquake Engineering 162 (2022) 107366. doi:10.1016/j.soildyn.2022.107366.

[13] X. Wang, S. Wan, P. Zhou, J. Fu, Z. Wu, Vibration mitigation in porous soil using periodic rock-socketed pile barriers, Soil Dynamics and Earthquake Engineering 171 (2023) 107956. doi:10.1016/j.soildyn.2023.107956.

[14] J. Avilés, F. J. Sánchez-Sesma, Piles as barriers for elastic waves, Journal of Geotechnical Engineering 109 (1983) 1133–1146. doi:10.1061/(ASCE)0733-9410(1983)109:9(1133).

[15] S. E. Kattis, D. Polyzos, D. E. Beskos, Vibration isolation by a row of piles using a 3-d frequency domain BEM, International Journal for Numerical Methods in Engineering 46 (1999) 713–728. doi:10.1002/(sici)1097-0207(19991020)46:5<713::aid-nme693>3.0.co;2-u.

[16] S. Brûlé, E. H. Javelaud, S. Enoch, S. Guenneau, Experiments on seismic metamaterials: Molding surface waves, Physical Review Letters 112 (2014) 133901. doi:10.1103/PhysRevLett.112.133901.

[17] A. Colombi, D. Colquitt, P. Roux, S. Guenneau, R. V. Craster, A seismic metamaterial: The resonant metawedge, Scientific Reports 6 (2016). doi:10.1038/srep27717.

[18] X. Pu, Z. Shi, Surface-wave attenuation by periodic pile barriers in layered soils, Construction and Building Materials 180 (2018) 177–187. doi:10.1016/j.conbuildmat.2018.05.264.

[19] Y. Zeng, Y. Xu, H. Yang, M. Muzamil, R. Xu, K. Deng, P. Peng, Q. Du, A matryoshka-like seismic metamaterial with wide band-gap characteristics, International Journal of Solids and Structures 185-186 (2020) 334–341. doi:10.1016/j.ijsolstr.2019.08.032.

[20] C. Zhao, C. Chen, C. Zeng, W. Bai, J. Dai, Novel periodic pile barrier with low-frequency wide bandgap for rayleigh waves, International Journal of Mechanical Sciences 243 (2023) 108006. doi:10.1016/j.ijmecsci.2022.108006.

[21] A. Hvatov, S. Sorokin, Assessment of reduced-order models in analysis of floquet modes in an infinite periodic elastic layer, Journal of Sound and Vibration 440 (2019) 332–345. doi:10.1016/j.jsv.2018.10.034.

[22] G. Floquet, Sur les équations différentielles linéaires à coefficients périodiques, Annales scientifiques de l'École Normale Supérieure 2e série, 12 (1883) 47–88. doi:10.24033/asens.220.

[23] F. Bloch, Über die quantenmechanik der elektronen in kristallgittern, Zeitschrift für Physik 52 (1929) 555–600. doi:10.1007/bf01339455.

[24] P. Mandal, S. N. Somala, Periodic pile-soil system as a barrier for seismic surface waves, SN Applied Sciences 2 (2020). doi:10.1007/s42452-020-2969-8.

[25] L. Meng, Z. Cheng, Z. Shi, Vibration mitigation in saturated soil by periodic pile barriers, Computers and Geotechnics 117 (2020) 103251. doi:10.1016/j.compgeo.2019.103251.

[26] A. Gupta, R. Sharma, A. Thakur, P. Gulia, Metamaterial foundation for seismic wave attenuation for low and wide frequency band, Scientific Reports 13 (2023). doi:10.1038/s41598-023-27678-1.

[27] G. Allaire, C. Conca, M. Vanninathan, The bloch transform and applications, in: M. Ahues, M. Boukrouche, C. Carasso (Eds.), ESAIM: Proceedings, volume 3, EDP Sciences, 1998, pp. 65–84. doi:10.1051/proc:1998040.

[28] P. G. Domadiya, E. Manconi, M. Vanali, L. V. Andersen, A. Ricci, Numerical and experimental investigation of stop-bands in finite and infinite periodic one-dimensional structures, Journal of Vibration and Control 22 (2016) 920–931. doi:10.1177/1077546314537863.

[29] M. Kadic, T. Frenzel, M. Wegener, When size matters, Nature Physics 14 (2017) 8–9. doi:10.1038/nphys4287.

[30] X. Zhou, Y. Xu, Y. Liu, L. Lv, F. Peng, L. Wang, Extending and lowering band gaps by multilayered locally resonant phononic crystals, Applied Acoustics 133 (2018) 97–106. doi:10.1016/j.apacoust.2017.12.012.

[31] S. del Broccolo, M. Ouisse, E. Foltete, F. Scarpa, Bandgap capability of hybrid kirigami inspired cellular structures, Advances in Aircraft and Spacecraft Science 6 (2019) 479–495. doi:10.12989/aas.2019.6.6.479.

[32] J. Huang, W. Liu, Z. Shi, Surface-wave attenuation zone of layered periodic structures and feasible application in ground vibration reduction, Construction and Building Materials 141 (2017) 1–11. doi:10.1016/j.conbuildmat.2017.02.153.

[33] Y. Achaoui, T. Antonakakis, S. Brûlé, R. V. Craster, S. Enoch, S. Guenneau, Clamped seismic metamaterials: ultra-low frequency stop bands, New Journal of Physics 19 (2017) 063022. doi:10.1088/1367-2630/aa6e21.

[34] J. Jensen, Phononic band gaps and vibrations in one- and two-dimensional mass–spring structures, Journal of Sound and Vibration 266 (2003) 1053–1078. doi:https://doi.org/10.1016/S0022-460X(02)01629-2.

[35] J.-P. Berenger, A perfectly matched layer for the absorption of electromagnetic waves, Journal of Computational Physics 114 (1994) 185–200. doi:10.1006/jcph.1994.1159.

[36] U. Basu, A. K. Chopra, Perfectly matched layers for time-harmonic elastodynamics of unbounded domains: theory and finite-element implementation, Computer Methods in Applied Mechanics and Engineering 192 (2003) 1337–1375. doi:10.1016/s0045-7825(02)00642-4.

[37] A.-S. Bonnet-Ben Dhia, S. A. Nazarov, Obstacles in acoustic waveguides becoming "invisible" at given frequencies, Acoustical Physics 59 (2013) 633–639. doi:10.1134/s1063771013050047.

[38] V. Pagneux, Trapped Modes and Edge Resonances in Acoustics and Elasticity, Springer Vienna, Vienna, 2013. doi:10.1007/978-3-7091-1619-7_5.

[39] A.-S. Bonnet-Ben Dhia, L. Chesnel, V. Pagneux, Trapped modes and reflectionless modes as eigenfunctions of the same spectral problem, Proceedings of the Royal Society A: Mathematical, Physical and Engineering Sciences 474 (2018) 20180050. doi:10.1098/rspa.2018.0050.

[40] S. Sorokin, P. Broberg, M. Steffensen, L. Ledet, Finite element modal analysis of wave propagation in homogeneous and periodic waveguides, International Journal of Mechanical Sciences 227 (2022) 107444. doi:10.1016/j.ijmecsci.2022.107444.

[41] L. Bourgeois, E. Lunéville, The linear sampling method in a waveguide: a modal formulation, Inverse Problems 24 (2008) 015018. doi:10.1088/0266-5611/24/1/015018.

[42] A. Recoquillay, Méthodes d'échantillonnage appliquées à l'imagerie de défauts dans un guide d'ondes élastiques, Phd thesis, Université Paris-Saclay, 2018.

[43] Z. Liu, X. Zhang, Y. Mao, Y. Y. Zhu, Z. Yang, C. T. Chan, P. Sheng, Locally resonant sonic materials, SCIENCE 289 (2000) 1734–1736. doi:10.1126/science.289.5485.1734.

[44] D. Chigrin, S. Enoch, C. S. Torres, G. Tayeb, Self-guiding in two-dimensional photonic crystals, Optics Express 11 (2003) 1203. doi:10.1364/oe.11.001203.

[45] W. Chew, Q. Liu, Perfectly matched layers for elastodynamics: a new absorbing boundary condition, Journal of Computational Acoustics 04 (1996) 341–359. doi:10.1142/S0218396X96000118.

[46] E. Garnell, O. Doaré, C. Rouby, Coupled vibro-acoustic modeling of a dielectric elastomer loudspeaker, The Journal of the Acoustical Society of America 147 (2020) 1812–1821. doi:10.1121/10.0000930.

[47] M. Miniaci, A. Krushynska, F. Bosia, N. M. Pugno, Large scale mechanical metamaterials as seismic shields, New Journal of Physics 18 (2016) 083041. doi:10.1088/1367-2630/18/8/083041.

[48] R. Zaccherini, A. Palermo, A. Marzani, A. Colombi, V. Dertimanis, E. Chatzi, Mitigation of Rayleigh-like waves in granular media via multilayer resonant metabarriers, Applied Physics Letters 117 (2020) 254103. doi:10.1063/5.0031113.